RSC Advances

PAPER

View Article Online
View Journal | View Issue

Cite this: *RSC Adv.*, 2024, **14**, 6216

Multifunctional modification polyester with Au@Cu_2O–ZnO ternary heterojunction fabricated by *in situ* polymerization

Mi Zheng,[a] Yong Jiang,[c] Cheng Wang,[a] Min Zheng *[a] and Zuoshan Wang *[b]

Received 26th December 2023
Accepted 4th February 2024

DOI: 10.1039/d3ra08856a

rsc.li/rsc-advances

In situ polymerization has been proven to be an effective method to introduce functional materials into polymers. In this work, a nano-heterojunction material was prepared successfully and evenly dispersed in PET by *in situ* polymerization methods to yield multifunctionally modified PET. The modified PET fibers showed excellent antibacterial activity and strong moisture absorption and perspiration, which could efficiently expel moisture from humans. Significantly, these prepared PET textiles demonstrate a strong safety without any cytotoxicity. Scanning electron microscopy (SEM) and transmission electron microscopy (TEM) revealed the uniform dispersion of heterojunctions and well-defined truncated octahedra including nano-gold rods. A series of characterizations including FTIR, XPS, XRD and DSC showed that the nano-heterojunction participates in the reaction during polymerization. It is interesting that the SEM images of the modified PET fiber presented an intriguing organ fold structure, which makes a significant contribution to moisture absorption and perspiration. The formation mechanism is discussed preliminarily.

1. Introduction

Chemical fibers have been widely used for their excellent physical and chemical properties. However, with the progress of science and technology and the further improvement of people's living standards, there is an increasingly widespread need to develop functional chemical fibers. Due to the characteristics of chemical fibers, in order to obtain a long-lasting function, the production method of functional chemical fibers is mainly based on blended spinning. For example, Chinese Patent No. 201510382672.8 provides a preparation method of antibacterial polyester fibers by blending PET polyester chips and antibacterial polyester masterbatch,[1] wherein the antibacterial polyester masterbatch is obtained by melting and extruding the mixture of PET polyester chips, antioxidants, lubricants and dispersing agents and pretreated nano-silver antibacterial agents. This solves the problem that nano-silver antibacterial agents with small particle sizes are poorly distributed in the PET matrix and can be generated from highly efficient and long-lasting antibacterial polyester fibers through melt-spinning. Due to the direct addition of nano-silver phosphate in the fiber as described in this document, the physical properties of PET are degraded, which will reduce the service life of the product. In other studies,[2,3] pre-prepared nanomaterials were dispersed directly into polymer monomers, and then mixed with other polymer monomers. In the above methods, the nanomaterial is not easily dispersed uniformly into the polymer monomer, and the particle size of the metal oxide is larger than 20 nm, which has a negative effect on the performance and blocks the materials while spinning. Some zinc-containing salts are also dissolved into polymer monomers and then polymerized with other monomers,[4,5] which has the disadvantage that the antibacterial properties of the products are still dependent on the release of zinc ions, due to the fact that the salts of these metals are simply mixed with the polymer and not incorporated into the polymeric structure. The concentration of the released zinc ions is controlled to be as low as possible to a lower level than legal limits. The migration of zinc ions cannot be avoided fundamentally. In addition, the as-prepared samples only have antibacterial function instead of multifunctions.

In recent years, with the development of medical and health undertakings, anti-bacterial multifunctional materials have been of interest to researchers. The dramatic increase in demand for personal protective equipment, including masks and gloves, has coincided with a significant rise in the quest for antimicrobial and multifunctional personal protective equipment.[6,7] Thus, the focus on polyester fabrics has gone beyond mere comfort, including health management functions, with a particular focus on their antimicrobial and moisture absorption and perspiration properties without security concerns. Copper-based heterostructured composite materials have many

[a]College of Textile and Clothing Engineering, Soochow University, Suzhou, Jiangsu 215123, China. E-mail: zhengmin@suda.edu.cn

[b]College of Material and Chemistry & Chemical Engineering, Soochow University, Suzhou, Jiangsu 215123, China. E-mail: zuoshanwang@suda.edu.cn

[c]Sichuan EM Technology Co., Ltd, No. 188 Sanxing Road, Mianyang 621000, China

advantages such as large storage capacity and easy preparation, and it is of practical significance to develop functional textiles based on these materials.[8–10]

Photocatalytic antibacterial technology has gained significant attention as a safe and effective antimicrobial technique. Unlike conventional approaches relying on metal ion leaching for bactericidal action, this process generates reactive oxygen species (ROS) through photocatalysis on semiconductor surfaces, effectively exterminating bacteria. This technology is expected to be a solution for the safe antimicrobial modification of polyester fibers.[11–13]

The integration of heterojunctions, combining diverse materials such as metals and semiconductor metallic oxides, offers promising prospects for improving photocatalytic performance. This stems from their ability to expand the spectral absorption range of a photocatalytic material and enhance charge carrier separation through favorable interface effects. Two notable photocatalysts, wide band gap zinc oxide (ZnO) (band gap of 3.2 eV) and narrow band gap cuprous oxide (Cu_2O) (band gap of 2.2 eV), have garnered attention for their exceptional photocatalytic efficacy, abundant availability, cost-effectiveness in synthesis, and low toxicity.[14,15] The strategic fabrication of ZnO/Cu_2O heterojunctions has emerged as a viable approach to achieve superior photocatalytic performance.[16] This configuration induces an irreversible electric field at the p–n interface, effectively suppressing the recombination of photoinduced electron–hole pairs.[17]

Herein, we prepared heterojunctions with uniform dispersion and well-defined truncated octahedra including nano-gold rods. Subsequently, we employed an *in situ* polymerization method to uniformly integrate the Au@Cu_2O/ZnO heterojunctions into PET fibers, resulting in excellent antibacterial activity and moisture absorption and perspiration without any cytotoxicity. Additionally, we thoroughly discuss the dispersity of nano-Au@Cu_2O/ZnO within the corresponding PET matrix and the consequential crystalline changes in the fabricated PET polymers. In particular, an exciting new development associated with moisture absorption and perspiration is the special organ fold structure in the modified fibers.

2. Experimental section

2.1 Materials

Ethylene glycol monomer and terephthalic acid were obtained from Jiangsu Hen-gli Chemical Fiber Group Co. Ltd, China. Copper acetate, zinc acetate, titanium sulfate, and polyvinyl pyrrolidone were purchased from Sinopharm Chemical Reagent Co. Ltd, China. All chemicals obtained from suppliers were used directly without further purification unless otherwise stated.

2.2 Preparation of Au@Cu_2O–ZnO

First, 0.1 g $CuCl_2$ was dissolved in 180 mL ultra-pure water, 2.02 g SDS was added and completely dissolved, 6 mL Au NRs solution and 6 mL NaOH (1 M) were added, and then 0.14 g hydroxylamine hydrochloride (10 mL aqueous solution) was added under rapid agitation. After precipitating for 2 h, filtration was carried out following water washing and alcohol washing. Au@Cu_2O was obtained finally through vacuum drying at 60 °C for 12 hours. The ternary heterojunction Au@Cu_2O@ZnO was obtained by an ultrasonic and microwave co-reactor through adding 0.06 g Au@Cu_2O nanopowder into a composite solution containing Zn^{2+} and stirring for 2 h with ultrasonication.

2.3 *In situ* synthesis of multifunctional polyester

Multifunctionality was realized by adding ternary heterojunction nanomaterials during the synthesis process. The ternary heterojunction Au@Cu_2O@ZnO was dispersed into ethylene glycol monomer under vigorous stirring and some modification agent was added to obtain precursor by reacting for 30 min in a microwave oven at 170 °C. Evaporating and concentrating the free water of the functional nano-oxide-containing polymer monomer under vacuum were conducted to control the water content below 2%. The obtained ethylene glycol monomer and terephthalic acid were added at a molar ratio of 1.2 : 1 to the polymer reaction vessel. Then 0.05% Sb_2O_3 and 0.02% triethyl phosphate (TEPA) were added at a mass ratio to the polymerization reactor, and the etherifying reaction carried out for 1 hour at a temperature of 200 °C and pressure of 2.0 MPa. Additionally, the mixture was heated to 270 °C to start the polymerization reaction for 2.5 hours. After the polymerization reaction was over, the product was spun, cooled, and shaped to obtain an anti-bacterial and moisture absorption and perspiration PET fiber.

2.4 Antibacterial evaluation

The antibacterial activity of PET/Au@Cu_2O–ZnO samples was evaluated against an array of two bacterial strains (obtained from the Microbial Type Culture Collection, MTCC), which are as follows: *S. aureus* (MTCC 96) as Gram-positive bacteria, and *Escherichia coli* (MTCC 443), as Gram-negative bacteria. The antibacterial rate was determined according to GB/T 23763-2009. Each experiment was assessed in triplicate, and all values are expressed as means ± standard error.

2.5 *In vitro* cytotoxicity tests

Safety evaluations of PET/Au@Cu_2O–ZnO fibers: the cytotoxicity of the as-prepared PET fiber was tested by biological evaluation of medical devices – part 5: tests for *in vitro* cytotoxicity (ISO 10993-5:2009). Cells were digested and suspended in culture medium. The cell concentration was adjusted to 1.0×10^5 mL^{-1}, and 100 μL cell suspension was inoculated into 96 well plates. After 24 hours of culture, the original culture medium was removed. 100 μL sample extraction solutions with different concentrations and a series of control samples were added to each well of the plate. After 24 hours of exposure in the incubator, 50 μL MTT solution was added to each well. After 3 hours of incubation in the incubator, the MTT solution was removed, and 100 μL isopropanol was added. The mixture was shaken in the dark for 10 minutes until the Jia Zan was completely extracted, and the absorbance value at a wavelength of 570 nm was measured using that of a blank well as a reference.

2.6 Moisture absorption and perspiration evaluations

The moisture absorption and perspiration evaluations of the textiles were conducted using the method for combination tests (GB/T 21655.1-2008). A commercial knitted fabric (COOLMAX cross fiber fabric) was used for comparison. Fabric specimens of different sizes were prepared for the tests. Before the test, the fabric was placed in an environment of (20 ± 2) °C and relative humidity of (65 ± 2)% for 24 hours. The concentration of each sample was measured five times, and the mean value was calculated. Moreover, the contact angle test was conducted for the demonstration of wettability.

2.7 Instruments and characterization

The microstructure and dimensions of the nano-heterojunction material were observed *via* a transmission electron microscope (TEM, FEI Tecnai G20). X-ray diffraction (XRD) patterns of the pure PET and PET/Au@Cu_2O–ZnO were collected using an X'Pert PRO powder diffractometer (Cu Kα radiation: 1.5406 Å; 40 kV, 40 mA) in the range of 5–80° 2θ scale. X-ray photoelectron spectroscopy (XPS, Thermo Fisher Scientific, USA) was conducted. The surface morphology of the fabric was observed by field-emission scanning electron microscopy (SEM, Regulus

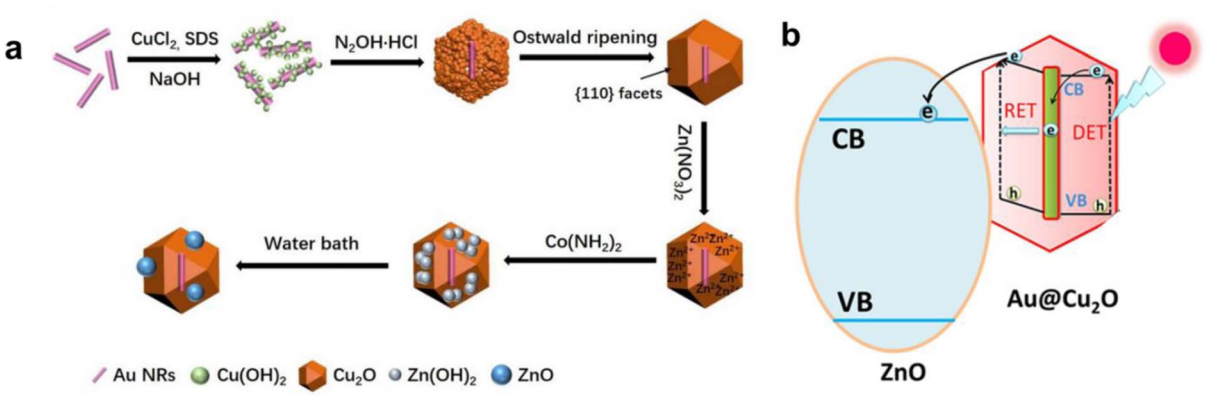

Fig. 1 Composite diagram (a) and electric transition diagram (b) of the Au@Cu_2O@ZnO ternary heterojunction.

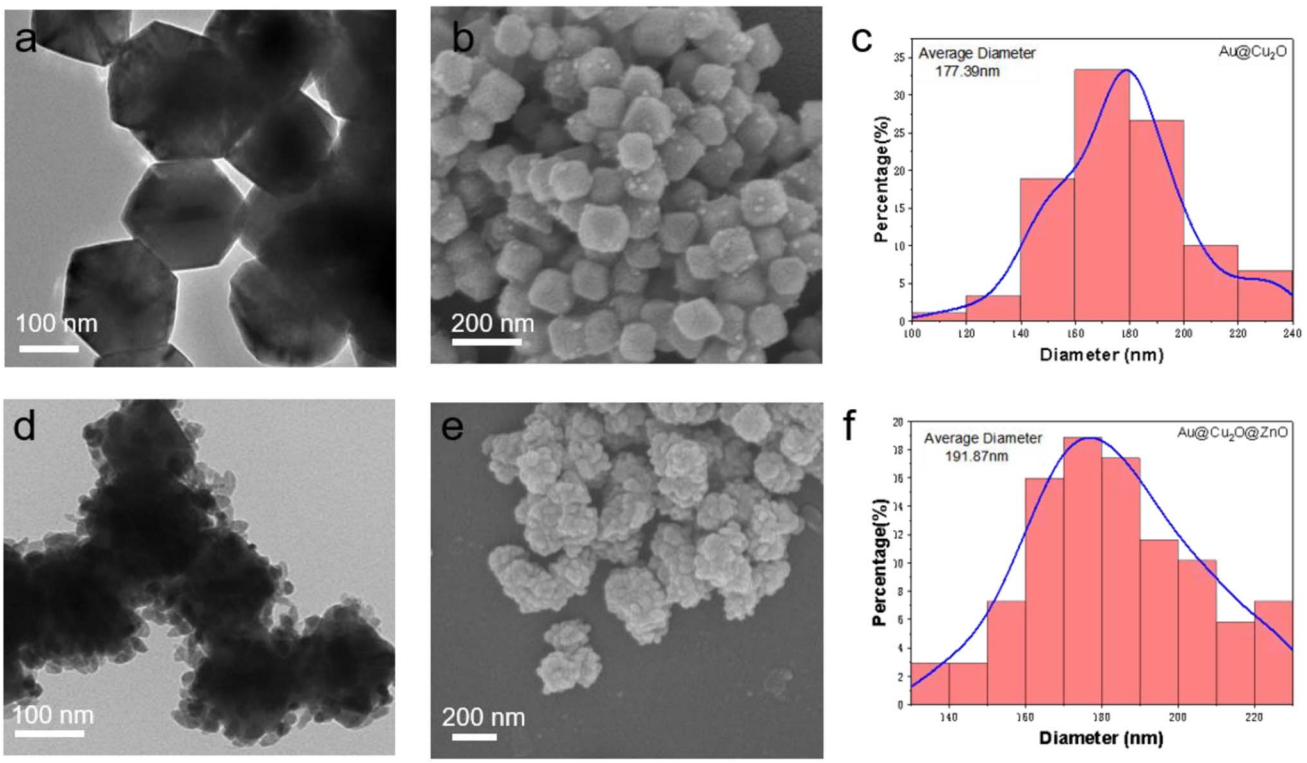

Fig. 2 (a) TEM image of binary heterojunction Au@Cu_2O. (b) SEM image of binary heterojunction Au@Cu_2O. (c) The average particle diameter of binary heterojunction Au@Cu_2O. (d) TEM image of Au@Cu_2O@ZnO ternary heterojunction. (e) SEM image of Au@Cu_2O@ZnO ternary heterojunction. (f) The average particle diameter of Au@Cu_2O@ZnO ternary heterojunction.

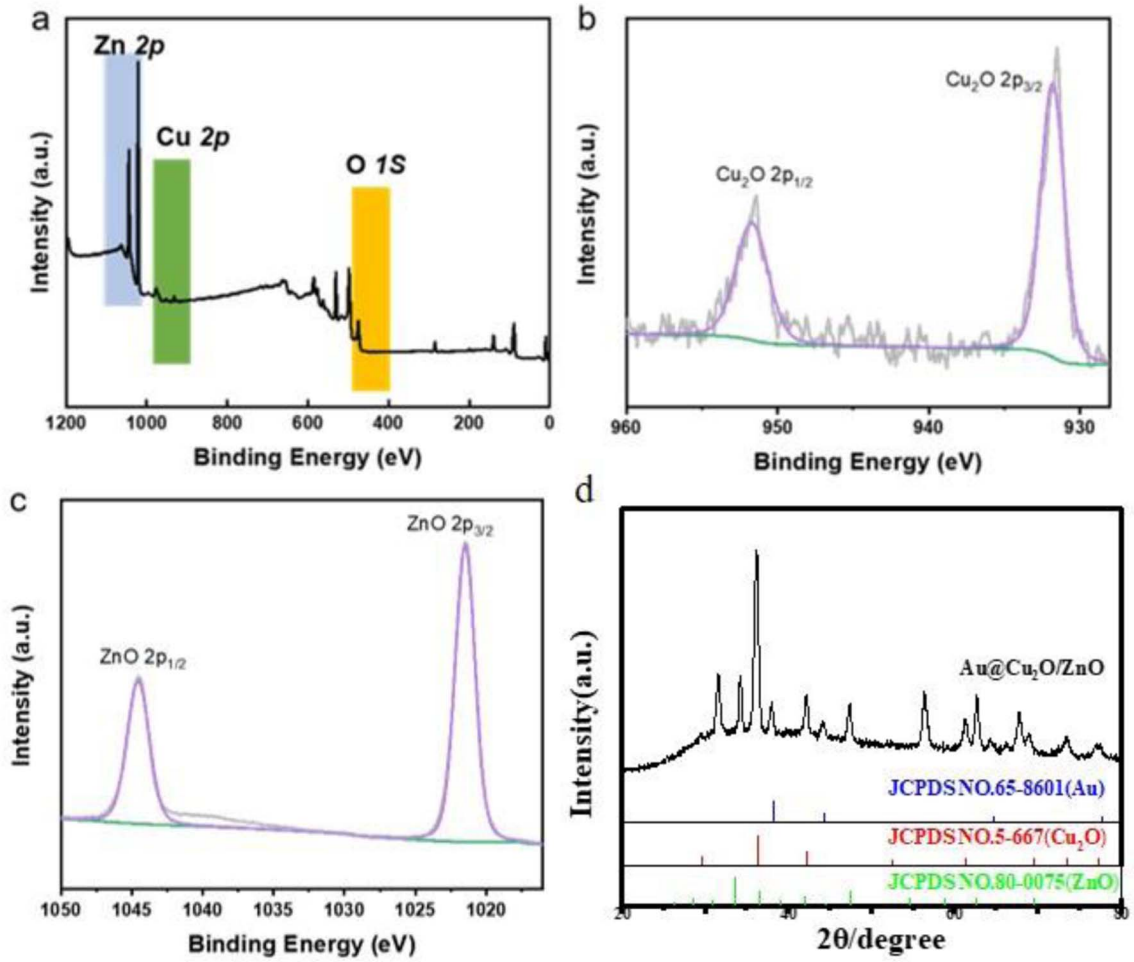

Fig. 3 (a–c) Component peak fittings of XPS spectra and (d) XRD pattern for Au@Cu_2O@ZnO ternary heterojunction.

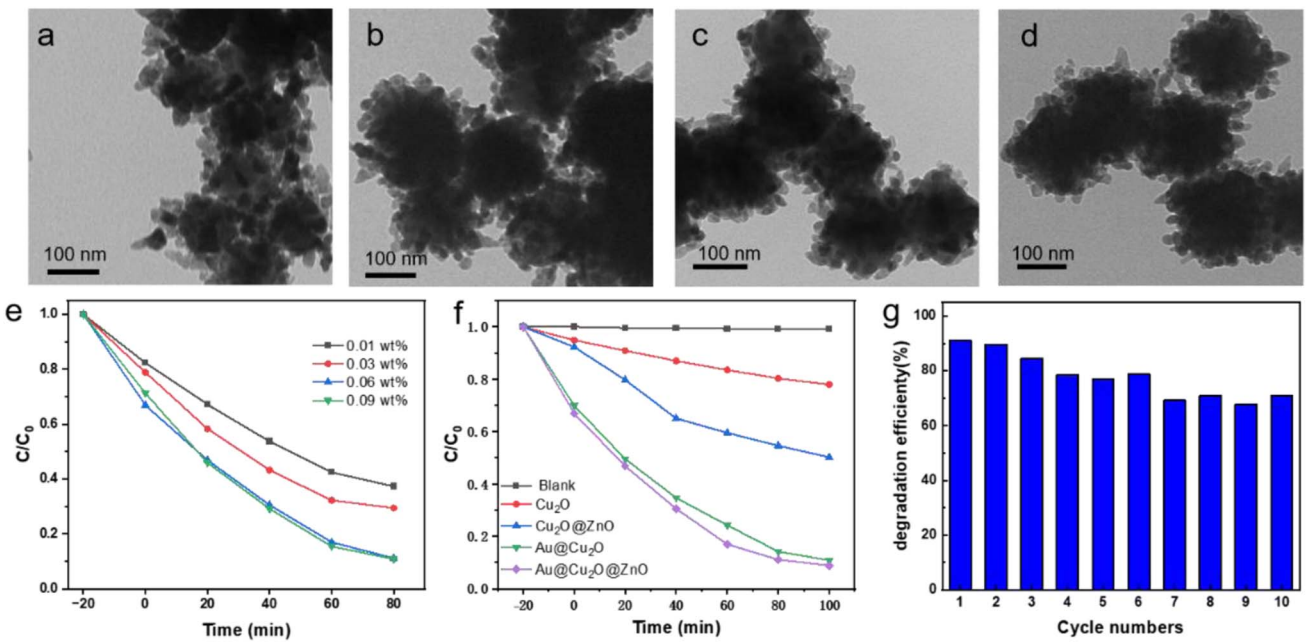

Fig. 4 Morphology modulation of Au@Cu_2O@ZnO ternary heterojunction with different mass fractions of Au@Cu_2O: (a) 0.01 wt% Au@Cu_2O; (b) 0.03 wt% Au@Cu_2O; (c) 0.06 wt% Au@Cu_2O; (d) 0.09 wt% Au@Cu_2O. (e) Photocatalytic degradation *versus* visible light irradiation time by using Au@Cu_2O@ZnO ternary heterojunction with different mass fractions of Au@Cu_2O. (f) Photocatalytic degradation *versus* visible light irradiation time by using different catalysts. (g) Photodegradation efficiency with cyclic testing.

8230). Fourier transform infrared analysis (Nicolet 6700 FTIR) was used for the analysis of molecular structure.

3. Results and discussion

3.1 Morphology of Au@Cu_2O–ZnO nanomaterials

The preparation process of the Au@Cu_2O–ZnO ternary heterojunction can be divided into two steps according to the composite diagram of the Au@Cu_2O@ZnO ternary heterojunction shown in Fig. 1: (1) preparation of Au@Cu_2O binary heterojunction and (2) preparation of Au@Cu_2O@ZnO ternary heterojunction. As shown in Fig. 2(a), the prepared Au@Cu_2O has a truncated octahedral structure with an average diameter of 177 nm. Au nanorods are wrapped with Cu_2O with regular edges. ZnO nanoparticles can be observed in Fig. 2(d). The small ZnO nanoparticles increased the roughness of the surface compared to the ternary heterojunction with an increased average diameter of 191 nm. XPS was performed to further confirm the synthesis of the heterojunction. XPS (Fig. 3) revealed the presence of Zn, Cu, and O. The high-resolution spectrum of Cu 2p is shown in Fig. 3(b), and the fitting peaks at 951.8 eV and 931.8 eV after fitting correspond to Cu^+ in Cu_2O. As shown in Fig. 3(c), the peaks centered at 1044.6 eV and 1021.5 eV correspond to ZnO $2p_{1/2}$ and ZnO $2p_{3/2}$, which confirmed that ZnO was successfully generated on the surface of Au@Cu_2O.

The coating state of zinc oxide is regulated by adjusting the added amount of binary heterojunction. As shown in the transmission electron microscopy images in Fig. 4(a–d), the less the addition amount of Au@Cu_2O, the more the ZnO coated on its surface. When the added amount reaches 0.06 wt%, the morphology changes are no longer obvious. The degradation curves of methyl orange with different added amounts Au@Cu_2O, as shown in Fig. 4(e), show that the degradation efficiency of methyl orange gradually increases with the increase of Au@Cu_2O addition and the increase is no longer obvious when the added amount is 0.06 wt%. This is because ZnO can be fully contacted with the increase of Au@Cu_2O. The methyl orange degradation curves of different materials for 100 min are shown in Fig. 4(f). Au@Cu_2O@ZnO showed better photocatalytic performance than binary Au@Cu_2O, and the methyl orange degradation efficiency reached 91.2% after 100 min, while that for Au@Cu_2O was 89.2%, which shows the introduction of ZnO enhanced the electron–hole separation effect and improved the photocatalytic performance. Au@Cu_2O@ZnO has excellent

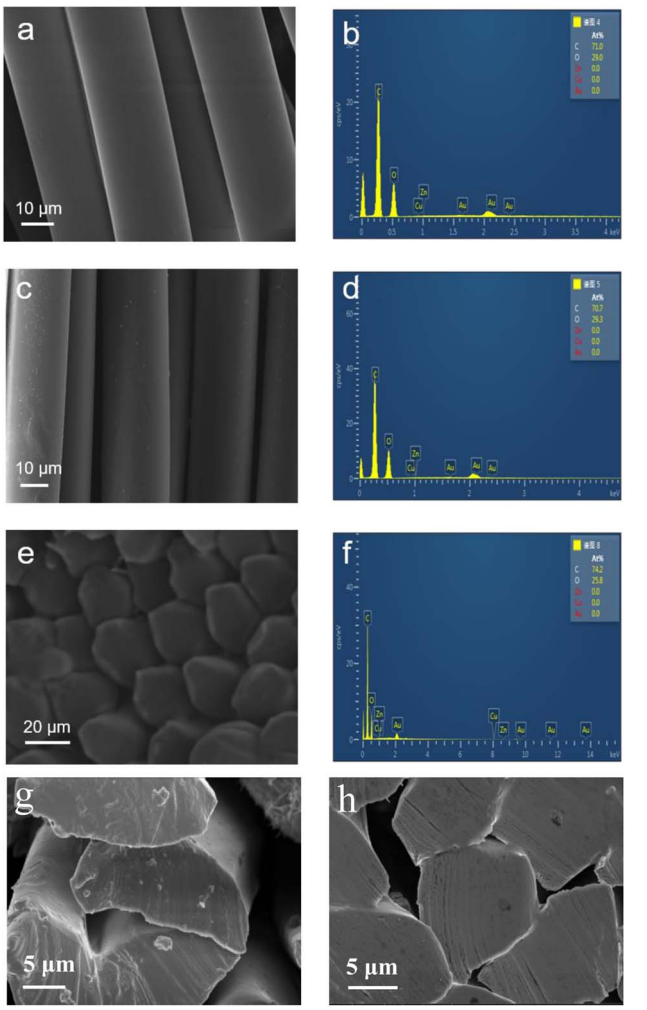

Fig. 5 SEM images and EDS traces of Au@Cu_2O@ZnO modified polyester. (a and b) SEM image and EDS of ordinary polyester. (c and d) SEM image and EDS of modified polyester. (e and f) SEM image and EDS of the cross section of modified polyester. (g and h) SEM images of the cross section at greater magnification of modified polyester and pure polyester.

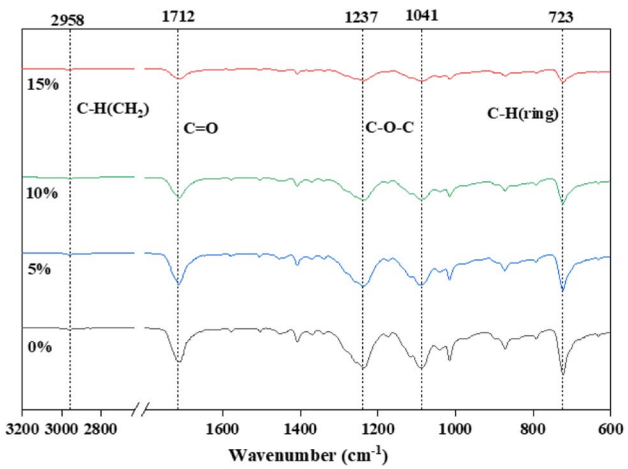

Fig. 6 FTIR spectra of PET and PET/Au@Cu_2O@ZnO polyester with different addition.

Table 1 C 1s XPS spectra of PET and PET/Au@Cu_2O@ZnO polyester with different addition

Sample	C–O–C	C=O	–CH_2–O	C–C
0 ppm	289.0	287.4	285.0	282.8
400 ppm	289.5	288.1	286.5	284.8
800 ppm	291.3	288.6	286.8	284.9
1200 ppm	291.8	288.9	287.5	284.9
Physical mixing	287.8	286.3	285.1	283.7

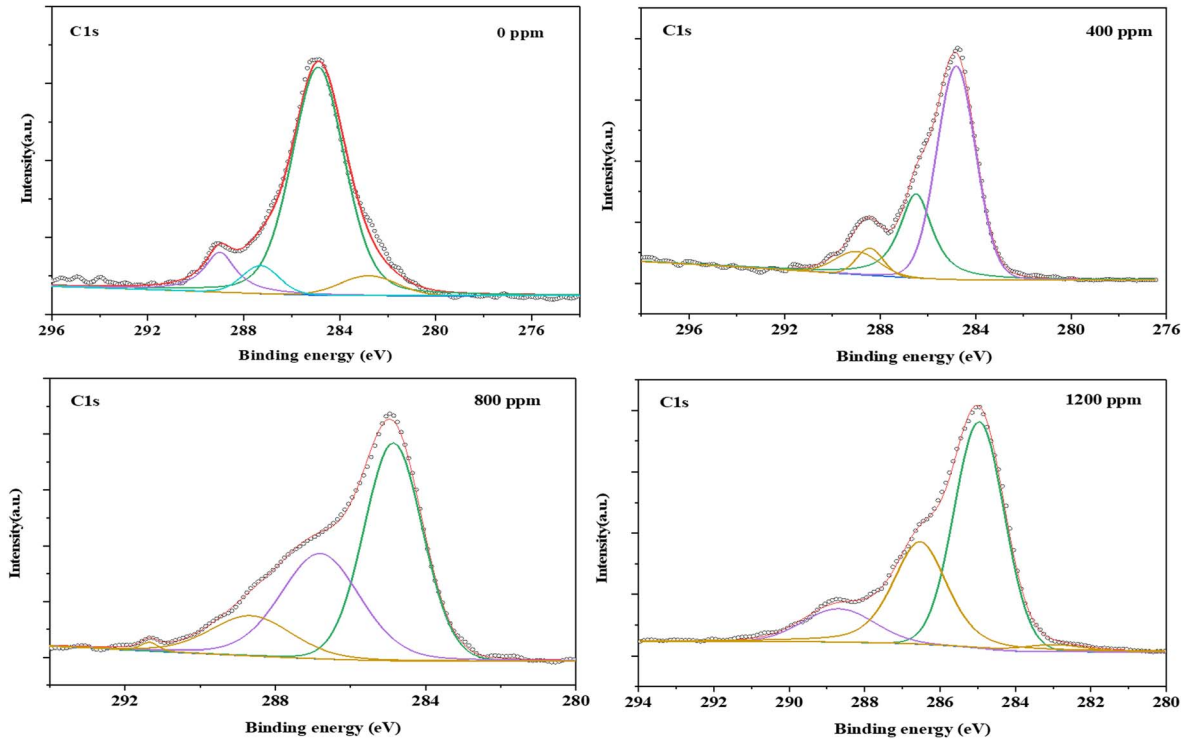

Fig. 7 C 1s XPS spectra of PET and PET/Au@Cu_2O@ZnO polyester with different addition.

photocatalytic stability, still maintaining 70% degradation rate of methyl orange after ten cycles of testing. This is due to the fact that the ZnO coating cuts off the contact between Cu_2O and air, which enhances its stability.

3.2 Characterization of the PET/Au@Cu_2O–ZnO composites

The interfacial compatibility of antibacterial agents in a polymer matrix significantly influences the properties of composite materials. Therefore, SEM was used to monitor the cross-section portion of the PET/Au@Cu_2O–ZnO composite, and the results are presented in Fig. 5(a–f). Remarkably, no noticeable differences were observed among the fracture sections of ordinary PET and PET/Au@Cu_2O–ZnO composites. All samples exhibited a homogenous phase, and no two-phase structure was evident in the PET/Au@Cu_2O–ZnO composites, indicating excellent dispersion of Au@Cu_2O–ZnO in the PET matrix. The strong complexation between metal ions and oxygen-containing functional groups in the heterostructured nanomaterials likely accounts for the robust interfacial compatibility.

Elemental analysis *via* EDS traces of modified polyester (Fig. 5d and f) clearly shows the existence of Au, Cu and Zn, indicating that there is a certain aggregation of nano-heterojunctions, which also indicates that Au@Cu_2O–ZnO is successfully loaded into the PET matrix.

Both PET/Au@Cu_2O–ZnO chips and fibers have been characterized. The characteristic peaks of modified PET are observed at 2958 cm^{-1} (–OH), 1712 cm^{-1} (C=O), 1237 cm^{-1} (C–O–C) and 1041 cm^{-1} (C–O–C) in the FT-IR spectra (Fig. 6 and Table 1). The strength of peaks at 1712 cm^{-1} and 1237 cm^{-1} became greater when more nanomaterials were added, which may be attributed to the strengthening of C=O tensile vibration coordinated interaction with metal ions. Similar changes were also observed in the XPS spectra. The C 1s peak (BE at 289.0 eV) from PET/Au@Cu_2O–ZnO shifted by 1.3 eV toward higher binding energies in comparison with pure PET, which was attributed to the ester C atoms. The integrated area of the carbonyl (C=O) peak also significantly increased with the peak position shifting from 287.4 eV to 288.9 eV (Fig. 7 and Table 2) due to the strong coordinate interaction between oxygen atoms

Table 2 O 1s XPS spectra of PET and PET/Au@Cu_2O@ZnO polyester with different addition

O 1s	OH	C–O–C	C=O
0 ppm	534.4	532.5	530.7
400 ppm	535.3	533.5	531.9
800 ppm	536.3	534.0	532.0
1200 ppm	536.8	534.4	532.8
Physical mixing	535.0	533.3	531.0

Table 3 Fiber tensile testing of yield strength and elongation at break for different addition

Sample (75D72F)	Yield strength (cN per dtex)	Elongation at break (%)
Pure PET	4.25	26.5
400 ppm Au@Cu_2O–ZnO/PET	4.30	21.5
800 ppm Au@Cu_2O–ZnO/PET	4.19	25.49
1200 ppm Au@Cu_2O–ZnO/PET	4.16	26.5

in oxygen functional groups and metal ions. Fiber tensile testing of yield strength and elongation at break for different addition shows that there is no effect on the stability (Table 3).

3.3 Evaluation of antibacterial activity and cytotoxicity of as-prepared PET/Au@Cu_2O–ZnO fiber

To evaluate antimicrobial performance, clinically isolated *Escherichia coli* (ATCC 25922, Gram-negative) and *Staphylococcus aureus* (ATCC 6538, Gram-positive) were tested. Fig. 8 and Table 4 show the antibacterial activity of ordinary PET and PET/Au@Cu_2O–ZnO composites against *Escherichia coli* and *Staphylococcus aureus* under dark and light condition for 24 h. As shown in Table 4, common PET showed no antibacterial activity against either type of bacteria. Lower concentration heterojunction of about 400 ppm leads to low antibacterial activity especially for *Escherichia coli* under dark environment. Above 800 ppm concentration of heterojunction, the composite exhibited excellent antibacterial activity under light condition, and especially for *Escherichia coli* under dark environment. The antibacterial properties of PET/Au@Cu_2O–ZnO composites were superior obviously under light *versus* dark conditions, which is consistent with heterojunction photocatalytic mechanisms. Antibacterial activity derives from electron–hole transitions, which require enough energy from excitation of ultraviolet or visible light, and follows the joint action of the photocatalytic antibacterial mechanism. The heterojunction structure design can significantly improve the antibacterial ability of nano-Cu_2O and ZnO, which indicates that the coaxial design with Au can effectively inhibit the recombination of electron and hole pairs, which is conducive to photocatalytic antibacterial properties.

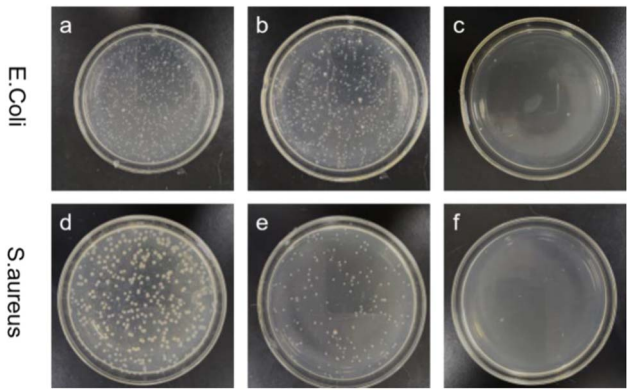

Fig. 8 Optical images of the antibacterial effect of Au@Cu_2O@ZnO-modified polyester: (a and d) control sample; (b and e) ordinary polyester; (c and f) Au@Cu_2O@ZnO-modified polyester.

Table 4 Antibacterial test against *Escherichia coli* and *Staphylococcus aureus* of different samples

		Antibacterial rate (%)	
Bacterium	Sample	Under light	No light
E. coli	PET	No effect	No effect
	PET/Au@Cu_2O–ZnO-400	18.72	24.28
	PET/Au@Cu_2O–ZnO-800	>99	95.36
	PET/Au@Cu_2O–ZnO-1200	>99	>99
S. aureus	PET	No effect	No effect
	PET/Au@Cu_2O–ZnO-400	52.31	26.68
	PET/Au@Cu_2O–ZnO-800	>99	74.4
	PET/Au@Cu_2O–ZnO-1200	>99	72.78

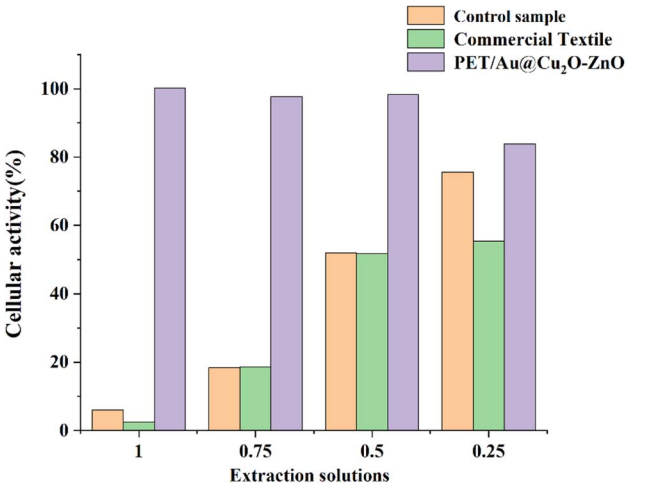

Fig. 9 Cytotoxicity of Au@Cu_2O@ZnO-modified polyester and commercially available antibacterial polyester.

Fig. 9 shows the cytotoxicities of the Au@Cu_2O–ZnO modified polyester and a commercially available antibacterial polyester. As shown in Fig. 9, the commercially available antibacterial polyester showed strong toxicity, and the cellular activity was only 2.49% for sample extraction solutions of 100% concentration. Surprisingly, the extraction solutions from the Au@Cu_2O–ZnO modified polyester not only have no toxicity, but also have higher activity than that of the blank sample, which can be attributed to the free oxygen generated by electronic transitions in ternary heterojunction nanomaterials. The zero cytotoxicity of the Au@Cu_2O–ZnO modified polyester also proves that Au@Cu_2O–ZnO is successfully loaded into the PET matrix.

3.4 Evaluation of moisture absorption and perspiration performance for PET/Au@Cu_2O–ZnO fiber

Table 5 and Fig. 10 show comparisons of moisture absorption and rapid drying performance between a knitted fabric developed from heterojunction *in situ* polymerized PET fibers and a commercial knitted product (COOLMAX cross fiber fabric) with the same specifications. From all indicators, it can be seen that the *in situ* polymerized polyester fibers have absolute advantages in moisture absorption and quick drying performance. Based on this, we have delved into the microstructure and mechanism of action. Fig. 11 shows SEM images of the cross section and surface of the Au@Cu_2O@ZnO modified polyester and ordinary polyester fiber. It can be clearly seen from Fig. 11 that there are many uniformly distributed nanoscale grooves on the fiber surface, which are interconnected and similar to organ folds, providing channels for water absorption

Table 5 Comparison of moisture absorption and rapid drying of Au@Cu_2O@ZnO-modified polyester with commercially available Coolmax polyester fiber with cross section

Test items	Modified sample	Coolmax sample	Standard requirements
Moisture absorption (%)	280	160	≥100
Dripping spread time (s)	≤1	≤3	≤3
Wicking altitude of direction (mm/30 min)	190	120	≥100
Wicking altitude of cross direction (mm/30 min)	195	140	≥100
Evaporation rate (g h^{-1})	0.36	0.26	≥0.18

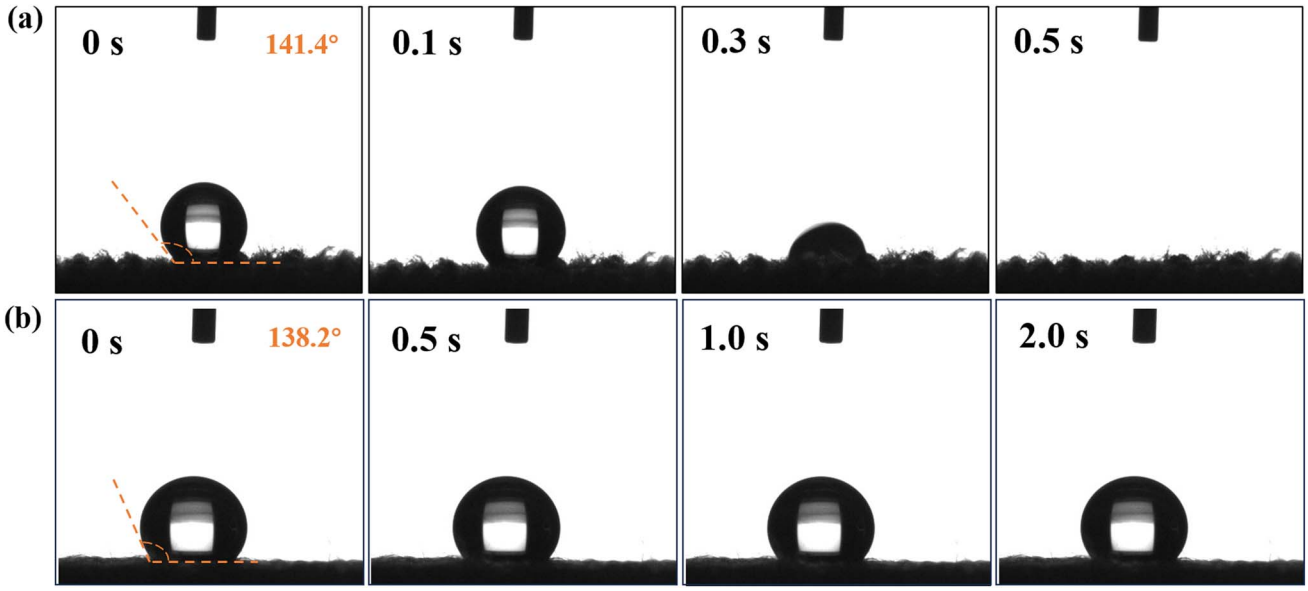

Fig. 10 The contact angle of water for Au@Cu_2O@ZnO-modified polyester fiber (a) and ordinary polyester fiber (b).

and transportation. Currently, there is no particularly clear mechanism for the formation of the organ folds. We speculate that it may be because of a special oligomer formed by the uniform migration of heterojunction modifiers to the surface during high-temperature spinning, and the specific formation mechanism needs further investigation.

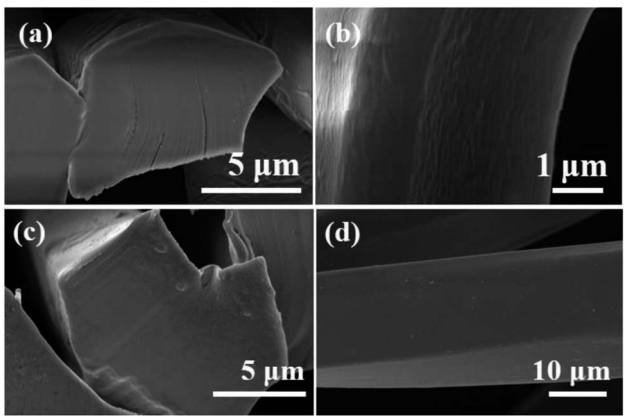

Fig. 11 SEM images of the cross section and surface of Au@Cu_2O@ZnO-modified polyester (a and b). SEM images of the cross section and surface of ordinary polyester (c and d).

4. Conclusions

In this work, a series of multifunctional modified PETs were prepared successfully *via in situ* polymerization by adding self-restrained ternary heterojunctions as antibacterial agents. SEM and TEM revealed the uniform dispersion of heterojunctions and well-defined truncated octahedra including nano-gold rods. A series of characterizations including FTIR, XPS, XRD and DSC showed that the heterojunctions participate in the reaction during polymerization. Scanning electron microscopy of the modified PET fiber showed an intriguing organ fold structure, which has a significant contribution to moisture absorption and perspiration. Antibacterial studies demonstrated strong *Escherichia coli* and *Staphylococcus aureus* inhibition under light condition. The modified PET fiber showed excellent antibacterial activity and strong moisture absorption and perspiration, which could efficiently expel moisture from a human. Significantly, the prepared PET textiles demonstrate a strong safety without any cytotoxicity. The formation mechanism was discussed preliminarily.

Author contributions

Mi Zheng: onceptualization, investigation, writing – original draft preparation; Yong Jiang: writing – original draft

preparation, investigation; Cheng Wang: data curation, investigation; Min Zheng: project administration, supervision; Zuo-Shan Wang: supervision; authors Mi Zheng and Yong Jiang contributed equally to this work.

Conflicts of interest

The authors declare no competing financial interest.

Acknowledgements

The authors acknowledge financial support from Jiangsu Naton Science & Technology Co. Ltd and the Multifunctional Material Collaborative Innovation Center of Soochow University (P110903419).

References

1 G.-J. Li, An antibacterial polyester fiber and its preparation method, CN2015103826728[P], 2015-07-01.
2 M.-F. Zhu, Antibacterial polyester fiber based on silver-containing zirconium phosphate, and method for reparation, WOCN2016/081472[P], 2016-08-14.
3 F. Micheleflori, N. Nocerina, R. Capparelli, *et al.*, Antibacterial polymers and method for obtaining the same, *US pat.*, 9527918B2, 2016-12-27.
4 F. Salaün, G. Lemort, C. Butstraen, E. Devaux and G. Capon, Influence of silica nanoparticles combined with zinc phosphinate on flame retardant properties of PET, *Polym. Adv. Technol.*, 2017, **28**(12), 1919–1928.
5 U. G. M. Ekanayake, K. Dayananda, N. Rathuwadu and M. Mantilaka, Fabrication of multifunctional smart polyester fabric *via* electrochemical deposition of ZnO nano-/microhierarchical structures, *J. Coat. Technol. Res.*, 2022, **19**(4), 1243–1253.
6 Y. W. Liu, C. H. Zhang, Z. Q. Wang, X. Fu and R. Wei, Scaly bionic structures constructed on a polyester fabric with anti-fouling and anti-bacterial properties for highly efficient oil–water separation, *RSC Adv.*, 2016, **6**(90), 87332–87340.
7 X. Zhang, W. S. Tong, F. Feng, Z. H. Wang, X. M. Wang and Y. H. Zhang, Polydopamine-assisted load of palygorskite on polyester fabric for moisture absorption and perspiration, *Appl. Clay Sci.*, 2022, **230**(15), 106720.
8 G. Ma, X. Liang, L. Li, *et al.*, Cu-doped zinc oxide and its polythiophene composites: Preparation and antibacterial properties, *Chemosphere*, 2014, **100**(3), 146–151.
9 M. Raffi, S. Mehrwan, T. M. Bhatti, *et al.*, Investigations into the antibacterial behavior of copper nanoparticles against Escherichia coli, *Ann. Microbiol.*, 2010, **60**(1), 75–80.
10 G. T. Yuan, M. N. Lu, J. H. Fei, J. Guo and Z. S. Wang, Morphologically controllable synthesis of core-shell structured Au@Cu_2O with enhanced photocatalytic activity, *RSC Adv.*, 2015, **5**(88), 71559–71564.
11 K. Varaprasad, G. M. Raghavendra, T. Jayaramudu, *et al.*, Nano zinc oxide–sodium alginate antibacterial cellulose fibers, *Carbohydr. Polym.*, 2016, **135**, 349–355.
12 Y. Y. Wang, M. Zheng, S. N. Liu and Z. S. Wang, Size Control and Growth Process Study of Au@Cu_2O Particles, *Nanoscale Res. Lett.*, 2016, **11**, 390.
13 Y. Su, H. Guo, Z. Wang, Y. Long, W. Li and Y. Tu, Au@Cu_2O Core-Shell Structure for High Sensitive Non-Enzymatic Glucose Sensor, *Sens. Actuators, B*, 2018, **255**, 2510–2519, DOI: **10.1016/j.snb.2017.09.056**.
14 S. Sun, Recent advances in hybrid Cu_2O-based heterogeneous nanostructures, *Nanoscale*, 2015, **7**, 10850.
15 S. Sun, X. Zhang, X. Yu, J. Cui, M. Yang, Q. Yang, P. Xiao and S. Liang, Unprecedented Ag–Cu_2O composited mesocrystals with efficient charge separation and transfer as well as visible light harvesting for enhanced photocatalytic activity, *Nanoscale*, 2021, **13**, 11867–11877.
16 S. Sun, L. He, M. Yang, J. Cui and S. Liang, Facet Junction Engineering for Photocatalysis: A Comprehensive Review on Elementary Knowledge, Facet-Synergistic Mechanisms, Functional Modifications, and Future Perspectives, *Adv. Funct. Mater.*, 2022, **32**, 2106982.
17 M. Zheng, A kind of anti-bacterial and anti-ultraviolet multifunctional chemical fiber, US11319647B2, 2020-06-09.